⌘ *Author's Choice*

A Glucose Transporter Can Mediate Ribose Uptake
DEFINITION OF RESIDUES THAT CONFER SUBSTRATE SPECIFICITY IN A SUGAR TRANSPORTER*

Christina M. Naula‡, **Flora M. Logan**‡, **Pui Ee Wong**‡, **Michael P. Barrett**‡§, and **Richard J. Burchmore**‡1

From the ‡Faculty of Biomedical and Life Sciences and §Wellcome Trust Centre for Molecular Parasitology, University of Glasgow, Glasgow G12 8QQ, Scotland, United Kingdom

Sugars, the major energy source for many organisms, must be transported across biological membranes. Glucose is the most abundant sugar in human plasma and in many other biological systems and has been the primary focus of sugar transporter studies in eukaryotes. We have previously cloned and characterized a family of glucose transporter genes from the protozoan parasite *Leishmania*. These transporters, called *Lm*GT1, *Lm*GT2, and *Lm*GT3, are homologous to the well characterized glucose transporter (GLUT) family of mammalian glucose transporters. We have demonstrated that *Lm*GT proteins are important for parasite viability. Here we show that one of these transporters, *Lm*GT2, is a more effective carrier of the pentose sugar D-ribose than *Lm*GT3, which has a 6-fold lower relative specificity (V_{max}/K_m) for ribose. A pair of threonine residues, located in the putative extracellular loops joining transmembrane helices 3 to 4 and 7 to 8, define a filter that limits ribose approaching the exofacial substrate binding pocket in *Lm*GT3. When these threonines are substituted by alanine residues, as found in *Lm*GT2, the *Lm*GT3 permease acquires ribose permease activity that is similar to that of *Lm*GT2. The location of these residues in hydrophilic loops supports recent suggestions that substrate recognition is separated from substrate binding and translocation in this important group of transporters.

Sugars are the primary energy currency for multicellular organisms, entering cells via transport systems that are critical for viability. Yet many unicellular organisms, including protozoan parasites, thrive in environments where sugar levels are low or variable. Glucose transport systems have been extensively studied in both humans and their parasites because this hexose is recognized as a key player in energy metabolism. Dysfunction in human glucose transport systems is implicated in pathologies such as obesity and diabetes, and glucose is the major sugar that is mobilized from mammalian energy reserves. Thus, characterization of glucose uptake has been a major research focus (1).

However, a diverse range of monosaccharide sugars is present in nature, and consequently monosaccharide sugars are of potential physiological importance to heterotrophic organisms. Transport systems for non-glucose monosaccharides have been described in bacteria (2) but are much less well understood in eukaryotes. For example, although the pentose sugar ribose is an important metabolic precursor and nutrient, no ribose transporter has been described at the molecular level from any animal.

In *Arabidopsis* (3), a polyol transporter has recently been cloned that has a broad specificity for sugars, including ribose. In yeast, pentose uptake is mediated by specific isoforms of the large family of hexose transporters (4). In mammalian cells, ribose uptake is partially blocked by the GLUT[2] inhibitor cytochalasin B, suggesting that ribose uptake may be mediated by members of the GLUT family of sugar transporters (5). The paucity of information about the uptake of ribose in eukaryotes arises, in large part, because the multiplicity of sugar transporters in higher organisms confounds attempts to isolate and characterize discrete transport activities. Simple eukaryotes, such as yeast (6) and protozoa (7, 8), also express multiple sugar transport systems that have significant sequence homology and strong structural similarity to their counterparts in mammals (9). Thus, functional analysis of any member of this transporter superfamily generates information that is broadly relevant.

Leishmania parasites encounter divergent habitats during their life cycle. The promastigote stage, which is adapted to life in the digestive tract of a sand fly vector, encounters a complex mixture of sugars that are derived from the plant-based diet of the insect host (10). Genetic ablation of glucose transport capacity profoundly affects the ability of *Leishmania* parasites to complete the insect vector phase of the life cycle (8). The amastigote stage is an obligate intracellular parasite of mammalian macrophages where it will likely encounter low glucose levels (11). Despite this, expression of a sugar transporter is essential for amastigote viability (8). Both promastigote and amastigote stages can accumulate (12) and metabolize (13) glucose, and glucose is the predominant sugar in the culture media that are used for axenic culture of both stages. Nevertheless, alternative sugars, such as ribose, may be encountered throughout the parasite life cycle (11) and can be utilized as a carbon source (14). Indeed, ribose may be essential for promastigote growth when glucose is absent (15). A saturable ribose uptake process has been described in *Leishmania donovani* with a K_m of 2 mM (16). This study concluded that ribose was transported by a system independent from the well characterized *Leishmania*

⌘ *Author's Choice*—Final version full access.
1 To whom correspondence should be addressed. Tel.: 44-141-330-8612; Fax: 44-141-330-4600; E-mail: r.burchmore@bio.gla.ac.uk.

2 The abbreviations used are: GLUT, glucose transporter; MFS, major facilitator superfamily; TM, transmembrane.

hexose transport system because ribose was unable to inhibit glucose or fructose uptake. Saturable ribose uptake has also been reported in *Leishmania mexicana* (17).

We have previously characterized a family of glucose transporters in *L. mexicana* called *Lm*GT1, *Lm*GT2, and *Lm*GT3 (18). These transporter isoforms are closely related in sequence but are expressed with unique temporal or spatial patterns. The most divergent member, *Lm*GT1, has a relatively low affinity for glucose and is localized specifically to the parasite flagellum. The biological relevance of this isoform is currently enigmatic. The other two members of the *Lm*GT family, *Lm*GT2 and *Lm*GT3, are greater than 90% identical, have a similar affinity for glucose, and are both expressed at the pellicular surface of the parasite. Both may contribute to glucose uptake, although *Lm*GT2 mRNA is significantly up-regulated in the promastigote stage. However, we report herein that *Lm*GT2 shows a greater capacity and affinity for ribose transport, a functional difference that must be mediated by the limited structural differences between *Lm*GT2 and *Lm*GT3.

Recently, we generated a glucose transporter knock-out mutant in *L. mexicana* (8) and have now exploited this null background to compare the substrate specificities of individual transport isoforms expressed in their native context. Herein we show that two very closely related transporters, called *Lm*GT2 and *Lm*GT3, have discrete substrate specificities. *Lm*GT2 binds a broader range of substrates and has a significantly higher affinity for ribose than does *Lm*GT3. Furthermore, by generation of chimeric transporters and extensive site-directed mutants, we localized specific motifs that are important for substrate discrimination. Our results are relevant to understanding substrate discrimination in related transporters of both parasites and their mammalian hosts.

EXPERIMENTAL PROCEDURES

Parasite Culture—*L. mexicana* WT MNYC/BZ/62/M379 and *L. mexicana* ΔGT mutant promastigotes were cultured at 25 °C in minimum Eagle's medium, designated HOMEM (19), containing 17 mM D-glucose and supplemented with 10% heat-inactivated FCS.

For the growth studies, cells were adapted to growth in SDM79 (20) containing 11 mM D-glucose and supplemented with 10% heat-inactivated FCS and then transferred to SDM80 (21) without glucose but supplemented with 10 mM ribose and 10% dialyzed heat-inactivated FCS. Growth studies were initiated at a density of 1×10^5 cells/ml, and cells were counted on an improved Neubauer hemocytometer.

Mutagenesis—*Lm*GT3 and *Lm*GT2 mutants were cloned in the *Leishmania* expression vector pX63Neo (22). Oligonucleotide-directed, site-specific *in vitro* mutagenesis was performed using the Stratagene site-directed mutagenesis QuikChange XL II kit. Mutations were confirmed by sequencing (MWG Biotech).

Generation of Transgenic Leishmania Cell Lines—*L. mexicana* ΔGT promastigotes were grown in culture to approximately 8×10^6/ml, washed in cold cytomix (0.15 mM $CaCl_2$, 120 mM KCl, 10 mM K_2HPO_4, 25 mM HEPES, 2 mM EDTA, 2 mM $MgCl_2$, pH 7.6), and resuspended in cytomix at 2×10^8/ml. 500-μl aliquots were electroporated in the presence of 10–20 μg of circular plasmid DNA (1.5 kV, 25 microfarads) using a Bio-Rad Gene Pulser II apparatus with 0.4-cm-electrode gap cuvettes and immediately transferred to 20 ml of HOMEM, 10% FCS. After 24-h incubation at 25 °C, cells were pelleted and resuspended in 10 ml of fresh HOMEM, 10% FCS with G418 (Calbiochem) at 50 μg/ml.

Confirmation of Genotype of Transgenic Leishmania Cell Lines—Transporter mutations in transgenic cell lines were confirmed by PCR and sequencing. Genomic DNA of transgenic parasites was isolated as follows. 5 ml of late log promastigote culture was pelleted, and the cells were washed once with phosphate-buffered saline pH 7.4 (PBS). Cell pellets were resuspended in 0.5 ml of lysis buffer (10 mM Tris-Cl, pH 8.0, 100 mM EDTA, 1% Sarkosyl, 100 μg of Proteinase K) and incubated at 50 °C overnight. The DNA was then extracted with 1 volume of phenol and 1 volume of chloroform. The aqueous phase was re-extracted with 1 volume of chloroform. The DNA was precipitated and resuspended in 100 μl of H_2O. The transgenic transporters were amplified from genomic DNA using GT2-specific primers 5′-TAGGTCCGAAAAGGAGCCC-3′ and 5′-GAAGCGAACATACAGCG-3′ or GT3-specific primers 5′-GAACTGGTTGTCCGAGG-3′ and 5′-GCACGCACACG-CACGTC-3′. The amplified products were sequenced by MWG Biotech to confirm the presence of the correct mutation in the transgenic cell lines.

Transport Assays—6-[^{3}H]Glucose (10–20 Ci/mmol) and 1-[^{3}H]ribose (10–20 Ci/mmol), supplied by Moravek Biochemicals Inc., were utilized for all transport assays. Mid- to late log phase *L. mexicana* promastigotes, transfected with *Lm*GT2, *Lm*GT3, or mutant constructs, were washed twice in PBS and resuspended in PBS to a final concentration of 3–5 × 10^8 cells/ml. Transport of radiolabeled ribose and glucose was measured at 25 °C with uptake found to be linear over 90 s for glucose and 6 min for ribose. The assays were terminated by spinning the cells in microcentrifuge tubes through an oil cushion of dibutyl phthalate/mineral oil (9:1) (Sigma) followed by immediate snap freezing in liquid nitrogen. The frozen cell pellet was clipped off into a scintillation vial, and 200 μl of 1% SDS was added. After 30 min, 4 ml of Optiphase HiSafe II scintillation mixture (PerkinElmer Life Sciences) was added. The samples were mixed, incubated overnight, and then analyzed by liquid scintillation counting.

Analysis of the data was performed using the software package Prism 5 (GraphPad Software Inc.). Transport kinetics were determined from replicate substrate saturation curves using the Michaelis-Menten equation ($n = 3$).

RESULTS

Molecular Basis of Ribose Transport in L. mexicana—We have previously reported that *L. mexicana* promastigotes express a saturable ribose transport system that is competitively inhibited by glucose but that a large excess of ribose was unable to block net glucose uptake measured in these cells (17). To investigate the possibility that one of the three functionally characterized *Lm*GT transporters might also mediate ribose uptake, we measured uptake of 0.1 mM ribose in *Lm*GT-null mutants that express individual *Lm*GT isoforms (Fig. 1*a*). *Lm*GT-null mutant promastigotes showed negligible ribose
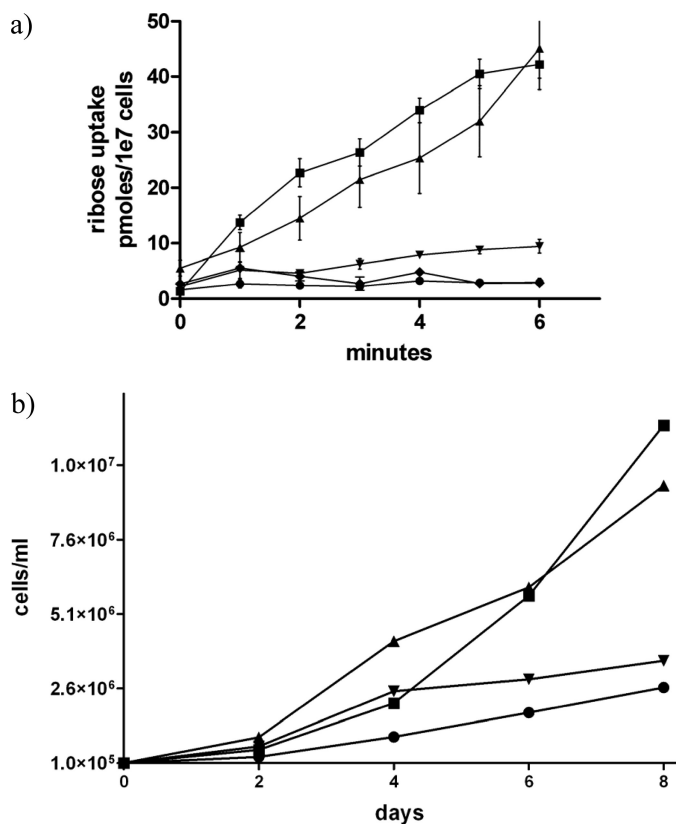
a)

b)

FIGURE 1. **Role of *Lm*GT2 and *Lm*GT3 in ribose acquisition by *L. mexicana*.** *a*, *Lm*GT2 is the main ribose transporter in *L. mexicana*. Promastigotes were incubated with 0.1 mM D-[³H]ribose. Ribose uptake was measured as described. Each *point* shows the mean of replicate assays with *error bars* showing S.D. (*n* = 3). ●, *L. mexicana* ΔGT; ■, *L. mexicana* wild type M379; ◆, *L. mexicana* ΔGT:pXNGT1; ▲, *L. mexicana* ΔGT:pXNGT2; ▼, *L. mexicana* ΔGT:pXNGT3. *b*, ribose can support growth of *L. mexicana*. Promastigotes were grown in SDM80 supplemented with 10 mM ribose. Each *point* shows the mean of duplicate cell counts. ●, *L. mexicana* ΔGT; ■, *L. mexicana* wild type M379; ▲, *L. mexicana* ΔGT:pXNGT2; ▼, *L. mexicana* ΔGT:pXNGT3.

uptake, whereas expression of *Lm*GT2 conferred ribose transport capacity that was similar to that observed in wild type promastigotes. Expression of *Lm*GT1 or *Lm*GT3 did not restore ribose uptake to wild type levels, suggesting that *Lm*GT2 is the major ribose transporter in *L. mexicana* promastigotes. We also tested the ability of *Lm*GT2 and *Lm*GT3 to support the growth of *Leishmania* in medium that contained ribose as the major carbon source and the only sugar (Fig. 1*b*). Wild type *Leishmania* promastigotes grew robustly in glucose-free medium supplemented with 10 mM D-ribose, albeit more slowly than in standard culture medium containing glucose (8). *Lm*GT-null mutant promastigotes grew poorly in glucose-free medium supplemented with 10 mM D-ribose. Expression of *Lm*GT2 permitted growth in medium containing 10 mM D-ribose at a rate similar to that observed for wild type promastigotes, but expression of *Lm*GT3 did not. This result clearly shows that *Leishmania* promastigotes can utilize ribose as a carbon source and, consistent with the evidence from ribose transport assays, indicates that *Lm*GT2 is the primary ribose transporter in *Leishmania*.

Nevertheless, *Lm*GT3 was able to mediate some ribose uptake. To quantify the relative ribose transport capacity of *Lm*GT2 and *Lm*GT3, we performed parallel glucose and ribose
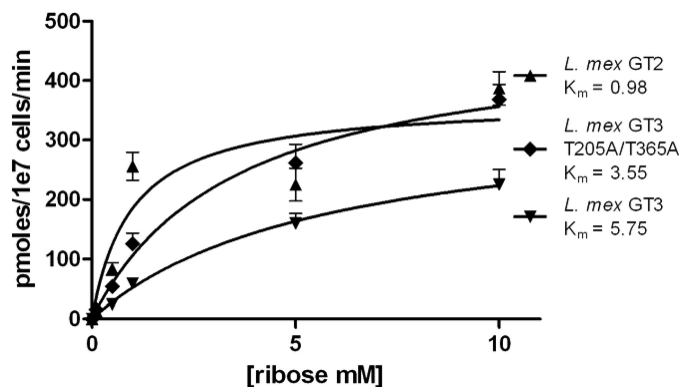

FIGURE 2. **Affinity for ribose uptake by Δ*Lm*GT:GT2, Δ*Lm*GT:GT3, and Δ*Lm*GT:GT3 double mutant T205A/T365A.** Promastigotes were incubated with various concentrations of D-[³H]ribose for 3 min during which the rate of uptake was linear. Ribose uptake was measured as described. Each *point* shows the mean of replicate assays with *error bars* showing S.D. (*n* = 3). *L. mex*, *L. mexicana*.

uptake assays in promastigotes expressing only *Lm*GT2 or *Lm*GT3. The initial rate of ribose uptake by *Lm*GT2 was 8-fold greater than the rate of ribose uptake by *Lm*GT3, although the rate of glucose uptake was similar in each. We measured a K_m for ribose uptake by *Lm*GT2 of 0.98 ± 0.31 mM, whereas the K_m for ribose uptake by *Lm*GT3 was 5.75 ± 2.11 mM (Fig. 2). *Lm*GT2 and *Lm*GT3 have a similar V_{max} for D-ribose transport (367 ± 32 and 352 ± 59 pmol/min/10⁷ cells, respectively). The specificity constant for ribose transport, indicated by the V_{max}/K_m ratio, is 6-fold greater for *Lm*GT2 than for *Lm*GT3 (V_{max}/K_m of 374 for *Lm*GT2 as opposed to 61 for *Lm*GT3).

Molecular Basis of Substrate Discrimination between LmGT2 and LmGT3—The predicted amino acid sequences of *Lm*GT2 and *Lm*GT3 are very similar (Fig. 3*a*), and the predicted topology is identical (Fig. 3*b*). The transporters are divergent at both amino and carboxyl termini. Internal to these divergent domains, there are only 12 amino acid differences. We performed systematic mutagenesis to generate a battery of full-length chimeric *Lm*GT mutants in which specific domains or residues were exchanged between the *Lm*GT2 and the *Lm*GT3 sequence. Throughout this work, mutant *Lm*GT constructs are systematically described with the *Lm*GT3 amino acid residue position, prefixed by single letter code for the *Lm*GT3 residue and suffixed by the *Lm*GT2 residue. All site-directed mutants are modifications of the *Lm*GT3 protein, replacing specific residues with the corresponding but divergent *Lm*GT2 residue. Mutant *Lm*GT transporters were expressed in *Lm*GT-null *L. mexicana* promastigotes, and the apparent rates of transport for glucose and ribose were measured by well established methods.

Amino-terminal Domain of LmGT2 Is Not Required for Ribose Transport—*Lm*GT2 and *Lm*GT3 differ primarily in their amino-terminal domain, and thus, we first investigated a potential role for this region in ribose transport. A chimeric *Lm*GT transporter, comprising the amino-terminal domain of *Lm*GT3 in place of the corresponding region in *Lm*GT2 (*Lm*GT3N/2), transported both glucose and ribose at a rate similar to that of wild type *Lm*GT2 (Fig. 4). The inverse construct, where the amino-terminal domain of *Lm*GT2 replaced the corresponding region in *Lm*GT3 (*Lm*GT2N/3), was able to

a)
```
                                                                    50
LmGT2  MSDKLEANGRSSRSEKEPIHDVITKNVMEDEDDAPPFLSASNARVTLVQA
LmGT3  MSDKLEANVQSSNWLSE-EPARPDANKLGDEDDSPPFFSMSNVRVAMVQA
                            TMD1
                                                                   100
LmGT2  IGGCLNGYSIGFVGVYSTLFGYSTNCANFRSERGCTTAPNADCQWFANAT
LmGT3  IGGCLNGYSIGFVGVYSTLFGYSTNCANFRSERGCTTAPNADCQWFANAT
                                        ◆
                                                                   150
LmGT2  GTSYCGWPEITCRRTYTYSSVAEMPGAIAQCEADSRCRWSYSAKECQNPS
LmGT3  GTSYCGWPEITCRRTYTYSSVAEMPGAIAQCEADSRCRWSYSAEECQNPS
                            TMD2
                                                                   200
LmGT2  GYSSSESGIFAGSMIAGCLIGSVFAGPLASTIGARLSFLLVGLVGVVSSV
LmGT3  GYSSSESGIFAGSMIAGCLIGSVFAGPLASTIGARLSFLLVGLVGVVSSV
         TMD3                     TMD4
                                                                   250
LmGT2  MCHVSASENEFWVLVVGRFVIGLFVGVIGVACPVYTDQNAHPKWKRTIGV
LmGT3  MYHVSTGENEFWVLVVGRFVIGLFVGVIGVACPVYTDQNAHPKWKRTIGV
                            TMD5
                                                                   300
LmGT2  MFQVFTTLGIFIAAAVGLALGQSTYFDRNKDQMVMARMQGLCAFSTLFSL
LmGT3  MFQVFTTLGIFIAAAVGLALGQSTYFDRNKDQMVMARMQGLCAFSTLFSL
                 TMD6
                                                                   350
LmGT2  LTILLGIVMSESRAKFGGDDEEGGIELDPNEYSYVEMVPRLLMGAVMAGT
LmGT3  LTILLGIVMSESRAKFGGDDEEGGIELDPNEYSYVEMVPRLLMGAVMAGT
          TMD7                     TMD8
                                                                   400
LmGT2  LQLTGINAVMNYAPAIMGSLGLAPLVGNFVVMLWNFVTTLASIPLSYVFT
LmGT3  LQLTGINAVMNYAPTIMGSLGLAPLVGNFVVMLWNFVTTLASIPLSYVFT
                            TMD9
                                                                   450
LmGT2  MRQLFLFGSLFTSSMCLFMCGIPVYPGVSKKTEVKNGVAITGILLFILGF
LmGT3  MRQLFLFGSLFTSSMCLFMCGIPVYPGVSKKTEVKNGVAITGILLFILGF
           TMD10                   TMD11
                                                                   500
LmGT2  EVCVGPCYFVLTQDMFPLSFRPRGASFTQVAQFIFNLIINVCYPIATEHI
LmGT3  EVCVGPCYYVLTQDMFPLSFRPRGASLTQVTQFLFNLVINVCYPIATEHI
                              TMD12
                                                                   550
LmGT2  SGGPSGNQDKGQAVAFIFFGCLGMICFIIQVFFLHPWDEKRDGKKRPATP
LmGT3  SGGLSGNQDKGQAVAFIFFGCVGMICFIIQVFFLHPWDEKRDGKKRPATP
              ◆              568
LmGT2  AGGKRELSSSLSGNRAE-
LmGT3  AGGKRELSGEFVGKKEV-
```
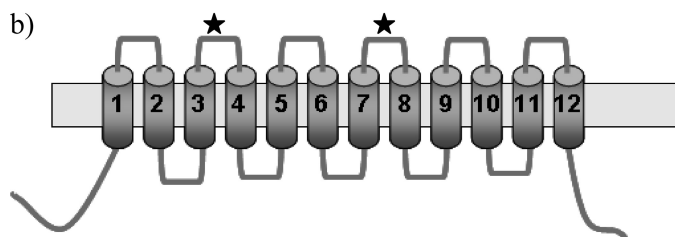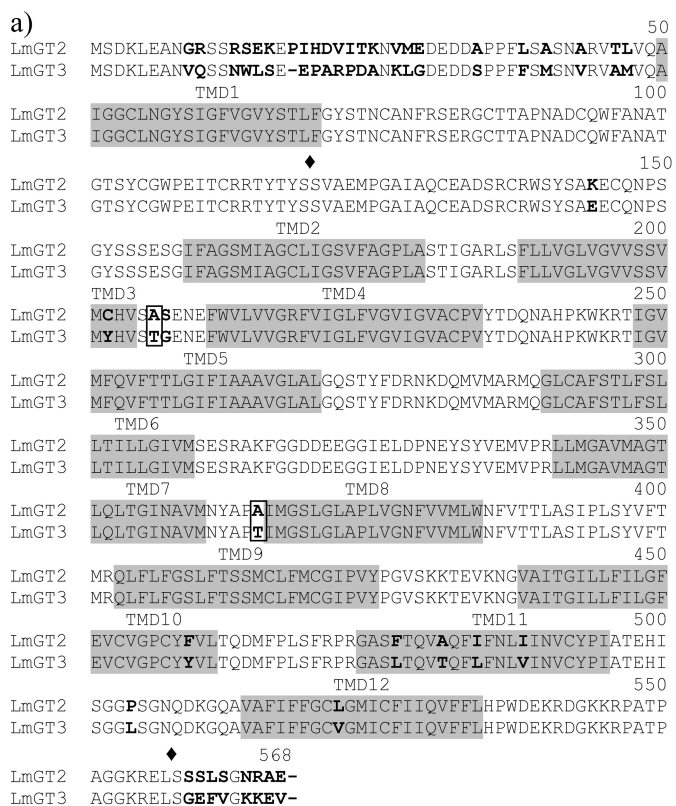
b)

FIGURE 3. Alignment of *Lm*GT2 and *Lm*GT3 and predicted topology. *a*, alignment of *Lm*GT2 and *Lm*GT3. Divergent amino acid residues are indicated in *bold*. Putative transmembrane domains (*TMD*), predicted by the TMHMM server, are *shaded* and *numbered*. Amino- and carboxyl-terminal chimera boundaries are indicated by ◆. Critical residues for discrimination between glucose and ribose are *boxed*. *b*, predicted topology of *Lm*GT3. *Stars* indicate the position of Thr-205 and Thr-365 in putative extracellularly oriented hydrophilic loops linking transmembrane domains 3 to 4 and 7 to 8.
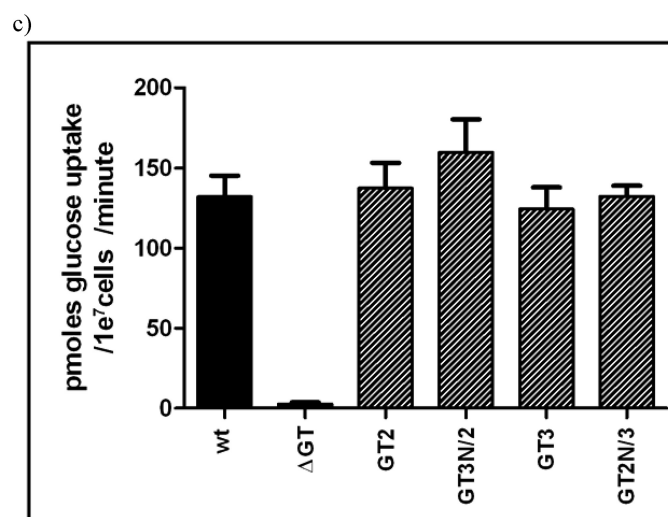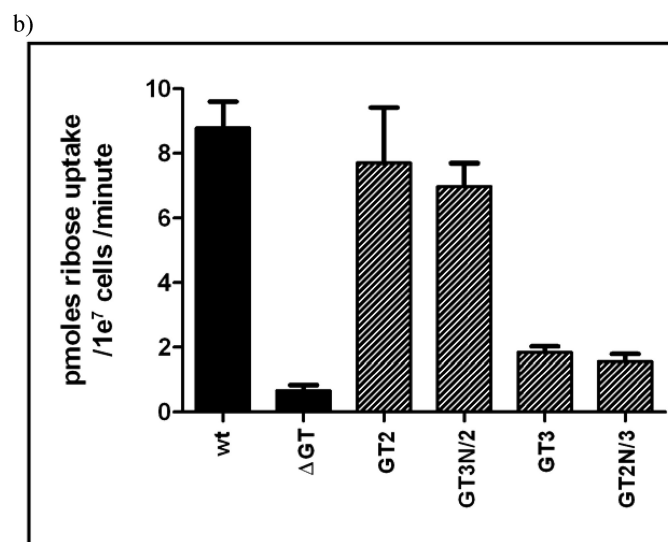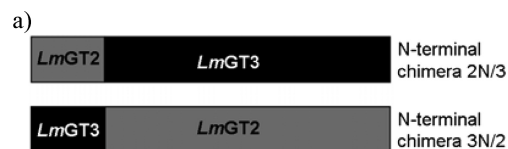
a)

b)

c)

FIGURE 4. Ribose and glucose uptake in amino-terminal chimeras. *a*, schematic of amino-terminal chimeras. *b*, ribose uptake in *L. mexicana* amino-terminal chimeras. Promastigotes were incubated with 0.1 mM D-[³H]ribose. Ribose uptake was measured as described over 3 min during which the rate of uptake was linear. Each *bar* shows the mean of replicate assays with *error bars* showing S.D. (*n* = 3). *GT2*, *L. mexicana* ΔGT:pXNGT2; *GT3N/2*, *L. mexicana* ΔGT:pXNGT3N/2; *GT3*, *L. mexicana* ΔGT:pXNGT3; *GT2N/3*, *L. mexicana* ΔGT: pXNGT2N/3. *c*, glucose uptake in *L. mexicana* amino-terminal chimeras. Promastigotes were incubated with 0.1 mM D-[³H]glucose. Ribose uptake was measured as described over 1 min during which the rate of uptake was linear. Each *bar* shows the mean of replicate assays with *error bars* showing S.D. (*n* = 3). *GT2*, *L. mexicana* ΔGT:pXNGT2; *GT3N/2*, *L. mexicana* ΔGT:pXNGT3N/2; *GT3*, *L. mexicana* ΔGT:pXNGT3; *GT2N/3*, *L. mexicana* ΔGT:pXNGT2N/3.

transport glucose at the same rate as either *Lm*GT2 or *Lm*GT3 but transported ribose at a rate similar to that of *Lm*GT3. This result clearly shows that the amino-terminal domain of *Lm*GT2 does not control discrimination between glucose and ribose substrates.

Carboxyl-terminal Domain of LmGT2 Is Not Required for Ribose Transport—A chimeric *Lm*GT transporter, comprising the carboxyl-terminal domain of *Lm*GT3 in place of the corresponding region in *Lm*GT2 (*Lm*GT3/2C), transported both glucose and ribose, whereas the inverse construct, where the carboxyl-terminal domain of *Lm*GT2 replaced the corresponding region in *Lm*GT3 (*Lm*GT2/3C), was able to transport glucose but transported ribose only weakly (Fig. 5). This result clearly shows that the carboxyl-terminal domain of *Lm*GT2 does not control discrimination between glucose and ribose substrates. Interestingly, replacement of the carboxyl-terminal domain of *Lm*GT3 with that of *Lm*GT2 generated a chimeric

protein (*Lm*GT3/2C) that transported both glucose and ribose at greater than double the rate observed for wild type *Lm*GT2, suggesting that sequences in the carboxyl terminus of *Lm*GT2 may be important for transporter activity.

Amino Acid Residues with Role in LmGT Substrate Specificity—Because neither the widely divergent amino or carboxyl termini could account for the ribose discrimination between GT2 and
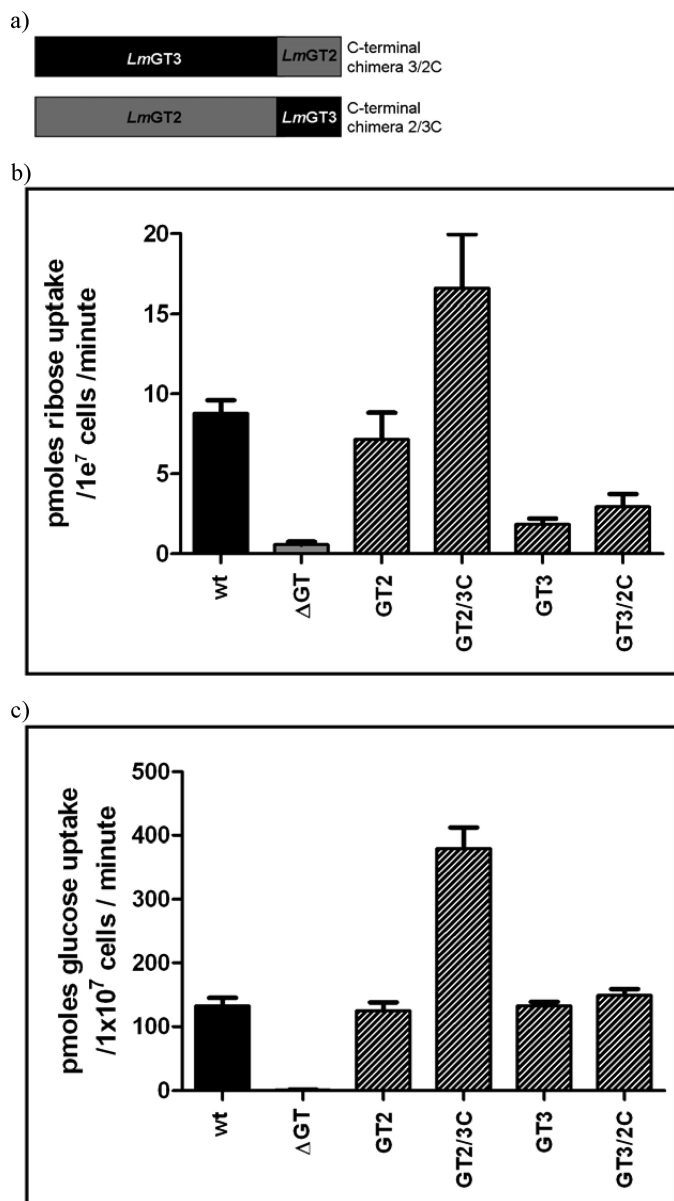
a)

b)

c)

FIGURE 5. **Ribose and glucose uptake in carboxyl-terminal chimeras.** *a*, schematic of carboxyl-terminal chimeras. *b*, ribose uptake in *L. mexicana* carboxyl-terminal chimeras. Promastigotes were incubated with 0.1 mM D-[³H]ribose. Ribose uptake was measured as described over 3 min during which the rate of uptake was linear. Each *bar* shows the mean of replicate assays with *error bars* showing S.D. (*n* = 3). *GT2*, *L. mexicana* ΔGT:pXNGT2; *GT2/3C*, *L. mexicana* ΔGT:pXNGT2/3C; *GT3*, *L. mexicana* ΔGT:pXNGT3; *GT3/2C*, *L. mexicana* ΔGT:pXNGT3/2C. *c*, glucose uptake in *L. mexicana* carboxyl-terminal chimeras. Promastigotes were incubated with 0.1 mM D-[³H]glucose. Ribose uptake was measured as described over 1 min during which the rate of uptake was linear. Each *bar* shows the mean of replicate assays with *error bars* showing S.D. (*n* = 3). *GT2*, *L. mexicana* ΔGT:pXNGT2; *GT2/3C*, *L. mexicana* ΔGT:pXNGT2/3C; *GT3*, *L. mexicana* ΔGT:pXNGT3; *GT3/2C*, *L. mexicana* ΔGT:pXNGT3/2C.

a)

b)

FIGURE 6. **Identification of residues responsible for substrate selectivity.** *a*, ribose uptake in single amino acid mutants (GT3 to GT2). Promastigotes were incubated with 0.1 mM D-[³H]ribose. Ribose uptake was measured as described over 3 min during which the rate of uptake was linear. Each *bar* shows the mean of replicate assays with *error bars* showing S.D. (*n* = 3). *Starred bars* are significantly different from GT3 ($p \leq 0.05$; *n* = 3). *b*, glucose uptake in single amino acid mutants (GT3 to GT2). Promastigotes were incubated with 0.1 mM D-[³H]glucose. Ribose uptake was measured as described over 1 min during which the rate of uptake was linear. Each *bar* shows the mean of replicate assays with *error bars* showing S.D. (*n* = 3). *Starred bars* are significantly different from GT2 ($p \leq 0.05$; *n* = 3).

GT3, we turned our attention to those residues that differentiate the transporters internally. A battery of site-directed mutants was generated to address the role in glucose and ribose transport of each of the internal amino acids that diverge between *Lm*GT2 and *Lm*GT3. All of these mutant *Lm*GT3 proteins exhibited robust glucose transport capacity, confirming that each is functionally expressed (Fig. 6*b*). This observation is unsurprising because each mutated residue is exchanged for
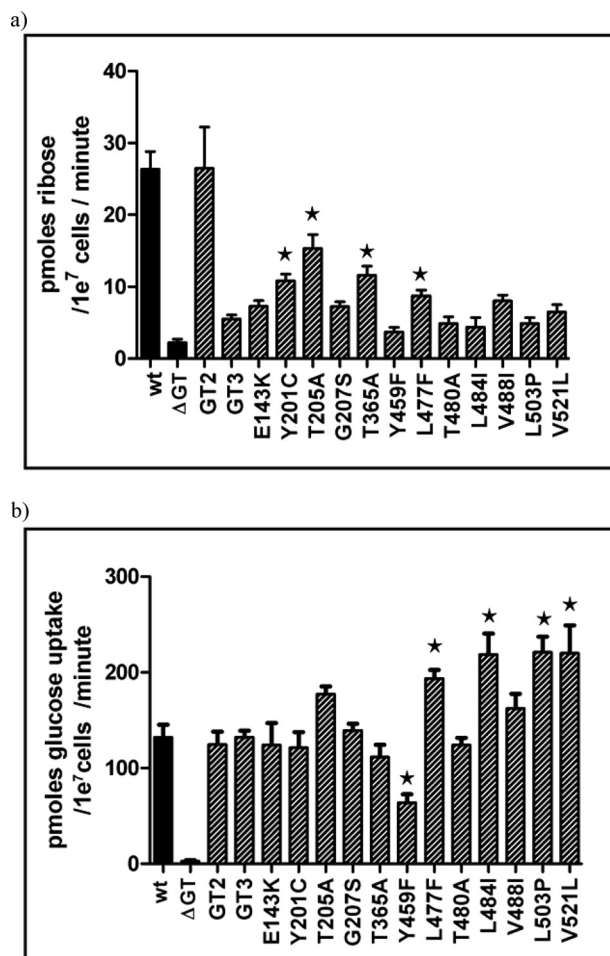
the corresponding residue in *Lm*GT2, which displays glucose transport characteristics similar to those of *Lm*GT3. However, several mutant *Lm*GT3 proteins showed augmented ribose transport capacity without individually creating a carrier whose ribose transporter capacity was equivalent to that of *Lm*GT2 (Fig. 6*a*). This indicates that multiple residues, working in concert, are responsible for differential substrate specificity. Ribose transport was significantly higher in *Lm*GT3 mutants Y201C, T205A, T365A, and L477F ($p \leq 0.05$; *n* = 3).

Structural Basis of Substrate Discrimination between LmGT2 and LmGT3—No structural information is available for *Lm*GT proteins, and high resolution structural data have been obtained only for very divergent prokaryotic MFS proteins (24, 25). Hydropathy analysis suggests that all MFS proteins have 12 transmembrane helices, and topology studies with MFS glucose transporters, particularly the archetypal human glucose transporter GLUT1, confirm this arrangement and demonstrate that both amino and carboxyl termini are cytoplasmically oriented

(26). Hydropathy analysis of *Lm*GT2 and *Lm*GT3 allowed prediction of the 12 likely transmembrane (TM) domains (Fig. 3) and enabled the topology of the divergent residues to be inferred. In addition to the divergent protein termini, clusters of divergent residues are located in TM11 and in the extracellular loop between TM3 and TM4, including the T205A mutation that alone confers greater than 50% of *Lm*GT2 ribose transport capacity on *Lm*GT3. An identical point mutation, T365A, is located in the relatively long extracellular loop that connects transmembrane domains 7 and 8 (Fig. 3*b*). We hypothesized that these divergent residues, although distant from one another in the *Lm*GT2 polypeptide chain, might interact in the transporter structure because they are located in flexible loops. We therefore generated two *Lm*GT3 mutants in which more than one residue was altered from the wild type sequence to the corresponding residue in *Lm*GT2 and assessed these mutants for the capacity to transport both glucose and ribose (Fig. 7).

Of these mutants, the double mutant T205A/T365A conferred upon *Lm*GT3 a ribose transport capacity of 6.8 pmol/10^7 cell/min, which was not significantly different ($p \leq 0.05$) from that measured for *Lm*GT2, 7.2 pmol/10^7 cell/min. The K_m for ribose transport by this mutant was 3.55 ± 0.93 mM, and the V_{max} was 483 ± 48 pmol/min/10^7 cells, giving a specificity constant of 136. Two amino acid residues that are located at the extracellular face of the protein structure are thus important to control discrimination between glucose and ribose in *Lm*GT.

DISCUSSION

Leishmania promastigotes are routinely cultivated in high concentrations of glucose. *Leishmania* encounter many other sugars during their life cycle (10, 27), but the utilization of these alternative carbohydrate energy sources has been largely overlooked. Most eukaryotes encode multiple putative glucose transporters (TransportDB), which may show different temporal and spatial expression patterns. An additional level of complexity may be conferred by postulating differential substrate specificities among structurally similar transporters. However, this possibility has proven more challenging to address because it requires functional expression of individual transporter isoforms in a null background. Although heterologous expression systems are frequently exploited to study transporter activity, the heterologous context may alter function. For this reason, we sought to exploit a glucose transporter-null *Leishmania* parasite as a homologous expression system for individual *Leishmania* glucose transporters.

Our present data show that *L. mexicana* promastigotes take up ribose via a membrane transporter, *Lm*GT2, that has previously been characterized as a hexose transporter. Although ribose is a ubiquitous sugar of central importance in metabolism, molecular characterization of ribose transport in a eukaryote has only recently been reported in plants (3). The demonstration that a hexose transporter of the major facilitator superfamily can also transport ribose is of general relevance.

Significant levels of ribose have been identified in analysis of the carbohydrate content of the sandfly vector of *Leishmania* (28). *Leishmania* can transport (16, 17) and metabolize (14)
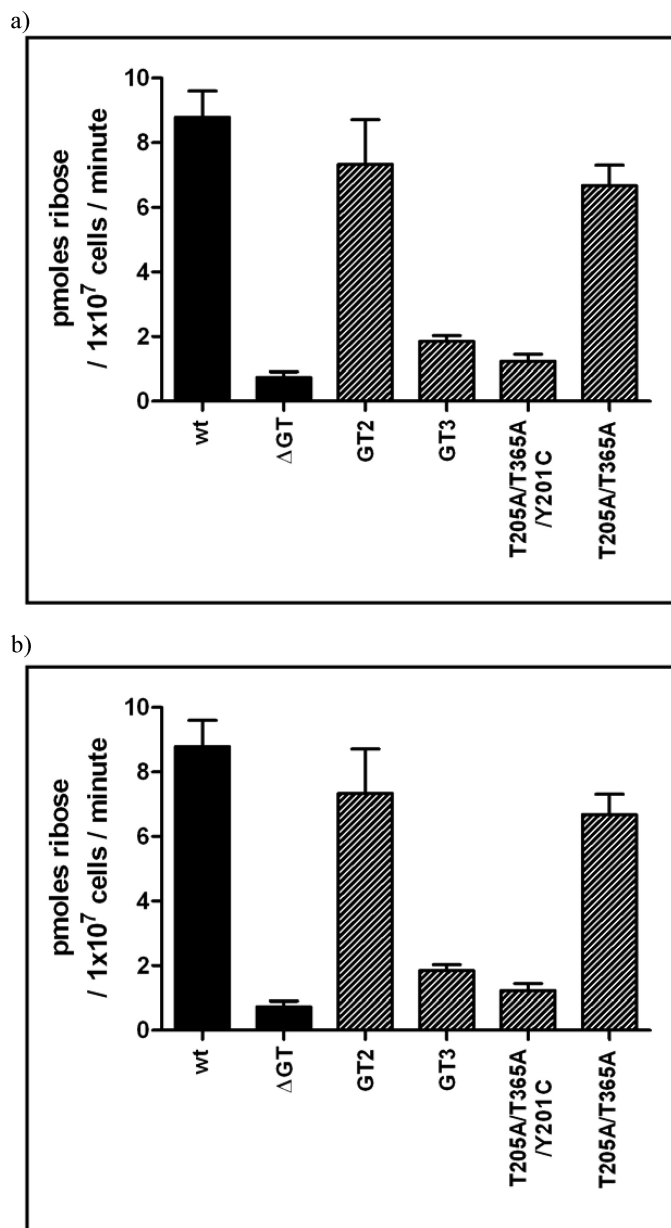

a)

b)

FIGURE 7. **Glucose and ribose transport in multiple mutants.** *a*, ribose transport in multiple amino mutants. Promastigotes were incubated with 0.1 mM D-[³H]ribose. Ribose uptake was measured as described over 3 min during which the rate of uptake was linear. Each *bar* shows the mean of replicate assays with *error bars* showing S.D. ($n = 3$). *GT2*, *L. mexicana* ΔGT:pXNGT2; *GT3*, *L. mexicana* ΔGT:pXNGT3; *T205A/T365A/Y201C*, *L. mexicana* ΔGT:pXNGT3 triple mutant (T205A/T365A/Y201C); *T205A/T365A*, *L. mexicana* ΔGT:pXNGT3 double mutant (T205A/T365A). *b*, glucose transport in multiple amino acid mutants. Ribose uptake was measured as described over 1 min during which the rate of uptake was linear. Each *bar* shows the mean of replicate assays with *error bars* showing S.D. ($n = 3$). *GT2*, *L. mexicana* ΔGT:pXNGT2; *GT3*, *L. mexicana* ΔGT:pXNGT3; *T205A/T365A/Y201C*, *L. mexicana* ΔGT:pXNGT3 triple mutant (T205A/T365A/Y201C); *T205A/T365A*, *L. mexicana* ΔGT:pXNGT3 double mutant (T205A/T365A).

ribose, and our unpublished data indicate that ribose can support growth of *Leishmania*. Ribose may also be an important energy source for the intracellular amastigote stage (11). We recently generated a hexose transporter-null *L. mexicana* mutant (8) and noticed that this line was also deficient in ribose transport. Results presented herein show that ribose transport is mediated most robustly by a specific isoform (*Lm*GT2) of the

*Lm*GT family of proteins, which have previously been characterized as glucose transporters (18).

*Lm*GT2 and *Lm*GT3 are membrane transport proteins that transport the hexose sugar glucose with similar affinity (109 ± 22 and 208 ± 40 μM, respectively). The proteins are very similar to each other in sequence but show functional differences (8, 18). Remarkably, *Lm*GT2 exhibits a higher affinity for the pentose sugar D-ribose (~1 mM compared with ~6 mM for *Lm*GT3), and the specificity constant (V_{max}/K_m) for ribose transport by *Lm*GT2 is ~6-fold greater than for ribose transport by *Lm*GT2. In addition, we have observed that glucose uptake via *Lm*GT2 is more sensitive to competitive inhibition by sugars such as fructose and 2,5-anhydromannitol (data not shown), which, like ribose, adopt a furanose conformation, whereas glucose is predominantly found in a pyranose conformation. We have investigated the molecular basis behind these functional differences using ribose transport capacity as a benchmark.

Transporter substrate specificity is rather poorly understood, but detailed study of the GLUT family of human facilitated hexose transporters to which the *Lm*GT proteins are homologous has enabled mapping of residues and domains that are important for function. In the absence of a defined structure, such studies have also elucidated much of the topology of the transporter protein (29). Structure-function analysis of a range of other MFS members suggests that topology is well conserved across the group, and the sequence homology between transporters from diverse organisms is very significant, particularly in predicted transmembrane helices (30).

Of the 12 TM helices that comprise GLUT1, helices 1, 2, 4, 5, 7, 8, 10, and 11 define a water-accessible cavity through which substrate must translocate. The recent definition of the three-dimensional structure of two MFS members (24, 25) supports this notion. Extensive scanning mutagenesis studies have assessed the importance to glucose transport of all the amino acid residues in transmembrane helices of GLUT1 (31), but there has been rather less focus on substrate selectivity and on the functional role of the hydrophilic loops. A QLS motif in helix 7 is important for discrimination between the pyranose glucose and the furanose fructose (32, 33), but these amino acids are unlikely to be directly involved in substrate discrimination because they are not exposed to the external solvent (31).

GLUT isoforms have been shown to transport a variety of hexose isomers and inositol (1). Recent analysis of substrate specificity in GLUT1 mutants (34) suggests that substrate binding involves sequential interaction with residues that line the aqueous pore from the cis- to the trans-opening. A substrate docking study with a GLUT1 homology model revealed the presence of a series of potential hexose binding sites along the pore (35), including a site at the outer rim that interacts with D-glucose but not with D-fructose. These data are consistent with passage of substrate through a hydrophilic pore by a multistage process that might act as a molecular filtering funnel. In this model of transporter function, substrate interacts sequentially with multiple binding sites rather than at a single site that can be alternately exposed on cis- and trans-sides of the lipid bilayer. Recent studies on the mechanism of substrate discrimination by GLUT transporters indicate that a residue near the exofacial end of the aqueous pore and remote from the translocation binding site is critical for distinguishing glucose from fructose (34, 37).

The limited regions of divergence between *Lm*GT2 and *Lm*GT3 are located in regions that have not previously been implicated in substrate discrimination. Our mutagenesis analysis reveals that neither the amino or carboxyl terminus nor most of the other divergent amino acids are important for discrimination of ribose from glucose. However, two alanine residues in *Lm*GT2, which are both substituted for threonine in *Lm*GT3, are together necessary and sufficient to convert *Lm*GT3 into a ribose transporter with capacity similar to that of *Lm*GT2. These amino acids are both located in extracellular hydrophilic loops and act synergistically to discriminate ribose from glucose. We propose that these residues comprise a substrate selectivity filter at the beginning of the substrate translocation pathway. Intramolecular interactions between the hydrophilic loop regions, which are often longer than is necessary to connect hydrophobic helices, may be important for substrate discrimination. Our data indicate that very subtle changes in amino acid sequence are sufficient to alter substrate specificity of a membrane transporter. In *Leishmania*, this may confer the ability to fine tune sugar transport capacity as it transits between different nutritional environments. A large number of related transporters that are expressed by mammals likely also display unique substrate specificities that have yet to be explored.

The majority of residues that diverge between *Lm*GT2 and *Lm*GT3 do not appear to play a role in discrimination between glucose and ribose. These divergences may underpin functional differences that have yet to be identified. The most prominent differences between the two isoforms are at the extreme termini, which are predicted to be cytoplasmically localized. Such regions may play roles in regulation of transporter localization (38, 39) or activity (23, 36), but here we demonstrate unambiguously that they are not responsible for differentiation between glucose and ribose. A remarkable group of four divergent residues in predicted TM11 are positioned such that they will be adjacent on a hydrophobic face of the helix (Fig. 3). A hydrophobic pocket, defined by TM11, is important for GLUT1 transport activity, and it is striking that each of these divergent amino acid positions conserves the hydrophobic character. In GLUT1, transmembrane helix 11 plays a key role in glucose binding. Individual or combined exchange of these divergent residues did not significantly alter transport of ribose or glucose (data not shown), raising the possibility that there may be further functional differences between *Lm*GT2 and *Lm*GT3.

Cells express membrane transporters that enable them to acquire hydrophilic compounds such as sugars while maintaining a permeability barrier with their environment. Transporter substrate specificity must therefore be adapted to the nutrient environment which, for *Leishmania* parasites, changes with life cycle progression. By expressing multiple structurally similar transporters that have discrete substrate specificities, *Leishmania* enhance their ability to exploit their hosts. Multiple isoforms of homologous membrane transporters are also expressed by mammals where their importance in energy metabolism and in various pathologies is recognized but not yet

well understood. Our current work demonstrates that relatively minor changes in transporter sequence can alter substrate specificity and supports the idea that substrate translocation involves sequential interactions. Structural definition of eukaryotic sugar transporters is currently a major research goal because these molecules are key targets for chemotherapy. However, elucidation of substrate specificity, which is important for the design of specific inhibitors, may also require functional studies of the kind reported here.

REFERENCES

1. Manolescu, A. R., Witkowska, K., Kinnaird, A., Cessford, T., and Cheeseman, C. (2007) *Physiology* **22,** 234–240
2. Iida, A., Harayama, S., Iino, T., and Hazelbauer, G. L. (1984) *J. Bacteriol.* **158,** 674–682
3. Klepek, Y. S., Geiger, D., Stadler, R., Klebl, F., Landouar-Arsivaud, L., Lemoine, R., Hedrich, R., and Sauer, N. (2005) *Plant Cell* **17,** 204–218
4. Sedlak, M., and Ho, N. W. (2004) *Yeast* **21,** 671–684
5. Lager, I., Fehr, M., Frommer, W. B., and Lalonde, S. (2003) *FEBS Lett.* **553,** 85–89
6. Bisson, L. F., Coons, D. M., Kruckeberg, A. L., and Lewis, D. A. (1993) *Crit. Rev. Biochem. Mol. Biol.* **28,** 259–308
7. Barrett, M. P., Tetaud, E., Seyfang, A., Bringaud, F., and Baltz, T. (1998) *Mol. Biochem. Parasitol.* **91,** 195–205
8. Burchmore, R. J., Rodriguez-Contreras, D., McBride, K., Merkel, P., Barrett, M. P., Modi, G., Sacks, D., and Landfear, S. M. (2003) *Proc. Natl. Acad. Sci. U.S.A.* **100,** 3901–3906
9. Saier, M. H., Jr., Beatty, J. T., Goffeau, A., Harley, K. T., Heijne, W. H., Huang, S. C., Jack, D. L., Jähn, P. S., Lew, K., Liu, J., Pao, S. S., Paulsen, I. T., Tseng, T. T., and Virk, P. S. (1999) *J. Mol. Microbiol. Biotechnol.* **1,** 257–279
10. Young, C. J., Turner, D. P., Killick-Kendrick, R., Rioux, J. A., and Leaney, A. J. (1980) *Trans. R. Soc. Trop. Med. Hyg.* **74,** 363–366
11. Burchmore, R. J., and Barrett, M. P. (2001) *Int. J. Parasitol.* **31,** 1311–1320
12. Burchmore, R. J., and Hart, D. T. (1995) *Mol. Biochem. Parasitol.* **74,** 77–86
13. Hart, D. T., Vickerman, K., and Coombs, G. H. (1981) *Mol. Biochem. Parasitol.* **4,** 39–51
14. Berens, R. L., Deutsch-King, L. C., and Marr, J. J. (1980) *Exp. Parasitol.* **49,** 1–8
15. Steiger, R. F., and Black, C. D. (1980) *Acta Trop.* **37,** 195–198
16. Pastakia, K. B., and Dwyer, D. M. (1987) *Mol. Biochem. Parasitol.* **26,** 175–181
17. Maugeri, D. A., Cazzulo, J. J., Burchmore, R. J., Barrett, M. P., and Ogbunude, P. O. (2003) *Mol. Biochem. Parasitol.* **130,** 117–125
18. Burchmore, R. J., and Landfear, S. M. (1998) *J. Biol. Chem.* **273,** 29118–29126
19. Berens, R. L., Brun, R., and Krassner, S. M. (1976) *J. Parasitol.* **62,** 360–365
20. Brun, R., and Schönenberger (1979) *Acta Trop.* **36,** 289–292
21. Lamour, N., Rivière, L., Coustou, V., Coombs, G. H., Barrett, M. P., and Bringaud, F. (2005) *J. Biol. Chem.* **280,** 11902–11910
22. LeBowitz, J. H., Coburn, C. M., McMahon-Pratt, D., and Beverley, S. M. (1990) *Proc. Natl. Acad. Sci. U.S.A.* **87,** 9736–9740
23. Bunn, R. C., Jensen, M. A., and Reed, B. C. (1999) *Mol. Biol. Cell* **10,** 819–832
24. Abramson, J., Smirnova, I., Kasho, V., Verner, G., Kaback, H. R., and Iwata, S. (2003) *Science* **301,** 610–615
25. Huang, Y., Lemieux, M. J., Song, J., Auer, M., and Wang, D. N. (2003) *Science* **301,** 616–620
26. Hresko, R. C., Kruse, M., Strube, M., and Mueckler, M. (1994) *J. Biol. Chem.* **269,** 20482–20488
27. Molyneux, D. H., Moore, J., and Maroli, M. (1991) *Parassitologia* **33,** (suppl.) 431–436
28. Cameron, M. M., Pessoa, F. A., Vasconcelos, A. W., and Ward, R. D. (1995) *Med. Vet. Entomol.* **9,** 263–272
29. Hruz, P. W., and Mueckler, M. M. (2001) *Mol. Membr. Biol.* **18,** 183–193
30. Manning, S. K., Woodrow, C., Zuniga, F. A., Iserovich, P., Fischbarg, J., Louw, A. I., and Krishna, S. (2002) *J. Biol. Chem.* **277,** 30942–30949
31. Mueckler, M., and Makepeace, C. (2009) *Biochemistry* **48,** 5934–5942
32. Arbuckle, M. I., Kane, S., Porter, L. M., Seatter, M. J., and Gould, G. W. (1996) *Biochemistry* **35,** 16519–16527
33. Seatter, M. J., De la Rue, S. A., Porter, L. M., and Gould, G. W. (1998) *Biochemistry* **37,** 1322–1326
34. Manolescu, A., Salas-Burgos, A. M., Fischbarg, J., and Cheeseman, C. I. (2005) *J. Biol. Chem.* **280,** 42978–42983
35. Cunningham, P., Afzal-Ahmed, I., and Naftalin, R. J. (2006) *J. Biol. Chem.* **281,** 5797–5803
36. Dauterive, R., Laroux, S., Bunn, R. C., Chaisson, A., Sanson, T., and Reed, B. C. (1996) *J. Biol. Chem.* **271,** 11414–11421
37. Manolescu, A. R., Augustin, R., Moley, K., and Cheeseman, C. (2007) *Mol. Membr. Biol.* **24,** 455–463
38. Snapp, E. L., and Landfear, S. M. (1997) *J. Cell Biol.* **139,** 1775–1783
39. Snapp, E. L., and Landfear, S. M. (1999) *J. Biol. Chem.* **274,** 29543–29548